Structure of human methaemoglobin: The variation of a theme

B. K. Biswal and M. Vijayan*

Molecular Biophysics Unit, Indian Institute of Science, Bangalore 560 012, India

There has been considerable interest in the variability of the structure of the liganded haemoglobin after characterization of the *R*2 state in addition to the original relaxed *R* state. The structures of three crystallographically independent relaxed haemoglobin molecules have been determined through the X-ray structure analysis of the crystals of human methaemoglobin. The three molecules have quaternary structures intermediate between those of the *R* and *R*2 structures. The same is true about the disposition of residues in the 'switch' region. Thus it would appear that haemoglobin can access different relaxed states with varying degrees of similarity among them.

HAEMOGLOBIN is among the most thoroughly studied proteins. Much of the current understanding of the allosteric mechanism has resulted from studies on haemoglobin[1,2]. Following the Monod, Wyman, and Changeux model[3], haemoglobin exists only in two states, corresponding to a low-affinity state called *T* and a high-affinity state called *R*. A stereochemical mechanism for the cooperative effects in the tetrameric protein was first proposed by Perutz[4] primarily on the basis of the deoxy[5] and met[6] forms of haemoglobin from horse. This mechanism, based on the equilibrium between the tense (*T*) deoxy state and the relaxed (*R*) liganded state, has stood the test of time[1], although new relaxed states have also been characterized recently[7–10].

Although the original studies that resulted in the elucidation of the mechanism of haemoglobin action were based on the protein from horse, structural investigations of haemoglobin from several vertebrates have been reported[2]. In particular, the focus of attention shifted to human haemoglobin. The crystal structures of oxy[11], deoxy[12] and carbonmonoxy[13,14] forms of the human protein have been studied. Those of the protein in liganded *T* states have also been reported[15,16]. The heme iron is ferrous in the *T* and *R* states. The iron is ferric and cooperativity is abolished in methaemoglobin. Surprisingly, no *R*-state human methaemoglobin structure has so far been reported. Although comparison of structures of human deoxyhaemoglobin with the structures of human carbonmonoxy and horse methaemoglobin has provided the necessary information for the rationalization of the allosteric mechanism[17], we have undertaken the X-ray structure analysis of human methaemoglobin to explore its similarity with different relaxed states. In the context of reports of subtle variations in molecular structure in the course of the action of haemoglobin, it is important to fully characterize the structure of the protein in all possible states. Here we report the crystal structure of human methaemoglobin, with three molecules in the crystal asymmetric unit.

Lyophilized powder of human methaemoglobin was purchased from Sigma Chemical Co and checked spectroscopically to ensure that the sample is fully met. The crystals were grown using the batch method from a 1 : 1 mixture of 25 mg/ml solution of protein in 0.01 M phosphate buffer, pH 6.7 and a 40% solution of PEG 4000 in the same buffer. The crystals grew in 1–2 weeks at room temperature.

A single crystal of dimensions $1.3 \times 1.2 \times 0.4$ mm mounted and sealed in a 1.5 mm glass capillary along with some mother liquor was used for data collection at room temperature on a 300 mm Mar image plate mounted on a RU200 Rigaku X-ray generator using CuKα radiation. The crystal to detector distance was set to 100 mm during data collection. The data were processed and scaled using DENZO and SCALEPACK[18]. The crystal data and data collection statistics are given in Table 1.

The structure was solved using the molecular replacement program AMoRe[19], with the structures of human oxyhaemoglobin[11] and horse methaemoglobin[20] as search models. Though both models gave the correct solution, the one obtained employing human oxyhaemoglobin was used for the eventual determination of the structure. The solution had a correlation coefficient of 0.342 and a *R*-factor of 0.446 and led to satisfactory packing, with three tetrameric molecules in the asymmetric unit. Structure refinement was carried out using CNS[21]. Fifty cycles of rigid body refinement treating each of the 12 subunits as a rigid body, led to a *R* of 0.336 and free *R* of 0.337. Also rigid body refinement was carried out treating the $\alpha\beta$ dimer as a rigid group. Eventually both approaches yielded the same result. The model was subjected to a 4000 K cartesian slow-cool protocol, using the maximum likelihood function as the target for refinement. At this stage a map was calculated and manual rebuilding was carried out using FRODO[22], wherever necessary. Grouped temperature factor refinement along with bulk solvent correction was used in all refinement cycles. R_{free} values were closely monitored throughout the refinement. Non crystallographic restraints (NCS) among the subunits of the same type in the asymmetric unit were applied from the beginning of the refinement. Cycles of position refinement and correction of model using Fourier maps were continued until no significant density was left in the map. Towards the end of the refinement an omit map[23] was calculated and used to remove model bias. The final model with three tetrameric molecules in the asymmetric unit has a

*For correspondence. (e-mail: mv@mbu.iisc.ernet.in)

R factor of 0.204 and a R_{free} of 0.245. The stereochemical acceptability of the structure was checked using PROCHECK[24]. The final model shows good stereochemistry with 86.0% of the total residues lying in the most favoured regions of the Ramachandran plot. An electron density map showing the heme region of the α subunit of molecule 1 is given in Figure 1. The refinement statistics are given in Table 1.

The primary objective of the present structure determination is, as mentioned earlier, the characterization of the subtle variations in the quaternary structure of liganded haemoglobin. It was therefore important to ensure that the final results do not suffer from model bias, particularly in view of the somewhat limited resolution of the diffraction data. Therefore, additional molecular replacement calculations were carried out using the human αβ dimer as the search model. The calculations did not yield definitive results, presumably because the search model accounted for only one-sixth of the scattering matter. Calculations were also carried out using the human $R2$ model, again without success. Molecules in the $R2$ structure were placed at the positions indicated by the molecular replacement solutions obtained using the oxyhaemoglobin model. The initial model containing molecules in the $R2$ state was then refined exactly in the same way as that containing oxyhaemoglobin molecules was refined. The refinement resulted in R and R_{free} of 0.211 and 0.262, respectively. The rms deviations in the C^{α} positions between the same tetramers in the two refined models were very low, at 0.22, 0.24 and 0.24 Å. The corresponding rms deviations in the side-chain atoms in the switch region (see later) were 0.37, 0.38 and 0.36 Å. The fact that refinements using two somewhat different models led to essentially the same results, testifies to their reliability.

Table 1. Data collection and refinement statistics. Values in parenthesis refer to the highest resolution shell (3.3–3.2 Å)

Data collection	
Space group	C2
Cell dimensions	a = 231.5, b = 57.9, c = 143.4 Å, β = 101.2°
Resolution (Å)	10–3.2
Number of reflections	
Total	84268
Unique	28048
Completeness	92.7 (63.0)
R merge	10.8 (37.9)
Refinement	
Resolution (Å)	10–3.2
Number of reflections	
Total	26690
Working set	25404
Test set	1286
Number of residues	1722
R (%)	20.4
R_{free} (%)	24.5
Deviations from ideal (rmsd)	
Bond distances (Å)	0.014
Bond angles (°)	1.3
Dihedral (°)	18.8
Improper (°)	1.1
Ramachandran plot	
% non-glycine or non-proline residues in most favoured regions	86.0
Additional allowed regions	13.2
Generously allowed regions	0.7
Disallowed regions	0.1

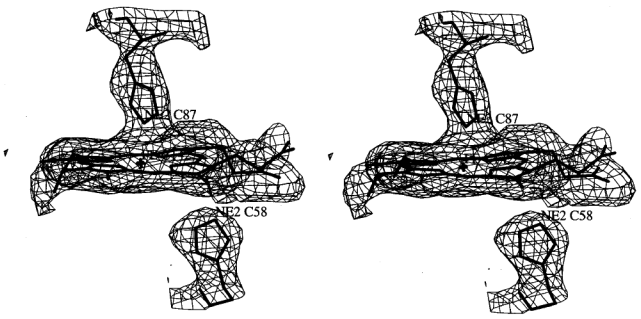

Figure 1. Stereo view of the electron density corresponding to the heme region of the α subunit in molecule 1 in the final $2Fo–Fc$ map. The contours are at 0.9 σ. The figure was generated using FRODO[22].

The present structure, that too with three crystallographically independent tetramers in it, is of particular interest in relation to the on-going discussion on different possible relaxed states of the molecule[2]. The crystals were grown at low ion concentration, a condition which has been suggested to favour a new relaxed state termed $R2$ (ref. 8). On the other hand, they were grown at the same pH as that used for crystallizing R state human oxyhaemoglobin[11] and not at a lower pH which favours the $R2$ state. Thus, the environmental conditions do not overly favour one or the other of the relaxed states. The attempt here is to compare the three tetrameric molecules in the structure with those in different known states with the help of the structural features that are widely used to characterize them.

To characterize the change in quaternary structure between pairs of structures under consideration as rigid body screw rotation[17], the following procedure was used. Each structure was transformed to a standard orientation in which the dyad relating α1β1 and α2β2 dimers was positioned along the Y-axis. The coordinates of the main-chain atoms of the α1β1 and α2β2 in each tetramer were averaged about the molecular dyad, to produce a tetramer with exact 2-fold symmetry.

The structure of the α1β1 subunit itself remains nearly the same in the different states. The difference between the tense and the relaxed states is primarily brought about by a movement of the α2β2 dimer as a whole with respect to the α1β1 subunit (Figure 2). A rough and ready estimate of this movement can be obtained by superposing the α1β1 dimers of a pair of

molecules and then calculating the rms deviations in the main-chain atoms for the $\alpha 2\beta 2$ dimer[8]. Such deviations between pairs of molecules among the relevant structures are given in Table 2. As shown by Baldwin and Chothia[17] and illustrated in Figure 2, the movements can be described in terms of a screw rotation angle (θ_2 in Figure 2), the screw rotation translation, the direction of the screw rotation axis and a point on the rotation axis. The same parameters can be used to describe the relationship between the quaternary structures of any two haemoglobin molecules. The values of all four parameters for pairs of different molecules are given in the lower left in Table 3. The first line of lower left in Table 3 corresponds to angle θ_2 and the translation (given in parenthesis). The second line indicates the direction of the rotation axis, whereas the third line defines a point on the rotation axis. Also given is the angle (θ_1) between axes that relates $\alpha 1\beta 1$ and $\alpha 2\beta 2$ dimers. The above calculations were done using the computer program 'align'[25].

As expected, the values in the left-bottom half of Table 2 clearly confirm that the internal structure of the $\alpha 1\beta 1$ dimer is substantially conserved with respect to variation in ligand-binding and species. Tables 2 and 3 also show considerable differences among the quaternary structures of the three crystallographically independent human methaemoglobin tetramers. Understandably, the quaternary structures of the three molecules are closer to those of human oxy[11], pig met[26] and horse methaemoglobin[20] than they are to those of the deoxy forms. However, the differences among the three

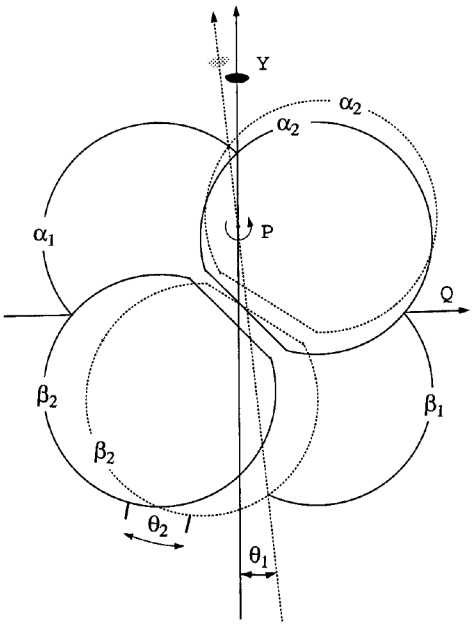

Figure 2. Schematic diagram showing the movement of $\alpha 2\beta 2$ relative to $\alpha 1\beta 1$ on going from unliganded (thick line) to liganded (dotted line) states. The movement involves a small translation along *P* as well. The figure has been adapted from figure 7 in Baldwin and Chothia[17].

are in some instances larger than those between one of them and one or the other of the remaining relaxed molecules under consideration.

In the context of the current discussion of the variability of the structure of the relaxed state of haemoglobin, it is of particular interest to compare the present structure with the *R* and the *R*2 forms of the molecule. The values of the rms deviation and the two angles, consistently show that molecule 3 of the met structure has a geometry very close to that of *R* state oxyhaemoglobin, while it exhibits the maximum deviation from the *R*2 structure. The same is true about molecule 2, but to a lesser extent. Molecule 1 is nearly, though not quite, as different from the *R* structure as it is from the *R*2 structure. The same trend in the relation between the three met molecules on the one hand and the molecules in the *R* and *R*2 states on the other, is exhibited by the translation (along with the rotation θ_2) that relates the $\alpha 2\beta 2$ dimer of one molecule and the $\alpha 2\beta 2$ dimer of another. Thus, the three tetramers in the met structure appear to represent states intermediate between *R* and *R*2, molecule 3 being the closest to the *R* structure and molecule 1, the farthest from it.

A region of the molecule that exhibits remarkable, functionally crucial differences between the tense and the relaxed structures, involves residues His97β2, Thr38α1, Thr41α1 and Pro44α1 in the $\alpha 1\beta 2$ interface (and their two-fold equivalent in the $\alpha 2\beta 1$ interface). This region is termed as the 'switch' region[17]. The disposition of the concerned residues in this region in the human deoxy, human *R*, human *R*2 and human met structures, is illustrated in Figure 3. In the deoxy *T* state, the side chain of the histidine residue is situated between Thr41α1 and Pro44α1 (not shown in the figure), while it is located between Thr38α1 and Thr41α1 in the *R* state. Steric hindrance prevents the smooth continuous movement of the histidyl side chain between the two locations. A switch of the residue between the locations involves a discrete change in the quaternary structure between *T* and *R*. In the *R*2 structure, His97β is farther away from the two threonyl residues and hence the steric hindrance to the movement between the two positions is not severe[8]. The distance between the C^{α} of His97β2 and Thr38α1 is 5.19 Å and 7.15 Å in the *R* and *R*2 structures, respectively. The corresponding distances in the met molecules 1, 2 and 3 are 6.96, 6.44, 6.01 Å, respectively. The similar distance involving Thr41α1 with His97β2 is 8.31, 8.40 and 8.30 Å in the three molecules as against 7.28 and 9.63 Å, respectively in the *R* and *R*2 states. On the whole, these distances also indicate the intermediate nature of the molecules of methaemoglobin in relation to those in the *R* and *R*2 states. This can be clearly seen in Figure 3 as well. In terms of interchain steric contacts involving the three residues, the molecules in the met state are probably closer to that in the *R*2 state. There are five such con-

Table 2. Rms deviations (Å) in the main-chain atoms resulting from the superposition of the α1β1 subunits of pairs of molecules. Those in the α1β1 subunits are given in the lower left and those in α2β2 subunits in the upper right

	1	2	3	4	5	6	7	8	9	10
1	–	1.30	2.63	3.01	3.23	2.41	3.16	6.42	7.15	6.07
2	0.14	–	1.44	2.10	3.53	1.65	2.38	6.25	6.95	5.83
3	0.26	0.25	–	1.30	4.61	1.13	1.51	5.78	6.39	5.28
4	0.64	0.63	0.71	–	4.73	0.87	1.06	5.08	5.27	4.67
5	0.58	0.54	0.66	0.43	–	3.93	4.81	8.85	9.57	8.22
6	0.60	0.61	0.66	0.50	0.55	–	1.17	4.98	5.56	5.61
7	0.63	0.63	0.65	0.57	0.63	0.50	–	4.48	4.98	4.39
8	0.73	0.79	0.78	0.75	0.71	0.61	0.76	–	0.83	1.03
9	0.78	0.84	0.81	0.74	0.78	0.75	0.75	0.83	–	0.98
10	0.85	0.91	0.91	0.84	0.89	0.79	0.85	0.65	0.64	–

1, Human met molecule 1 (PDB code: 1JY7, resolution: 3.2 Å); 2, Human met molecule 2; (1JY7, 3.2 Å); 3, Human met molecule 3 (1JY7, 3.2 Å); 4, Human oxy (1hho, 2.1 Å); 5, Human *R*2 (1bbb, 1.7 Å) ; 6, Horse met (2 mhb, 2.0 Å); 7, Pig met (2pgh, 2.8 Å); 8, Human deoxy (2hhb, 1.7 Å); 9, Human deoxy low salt (1hbb, 1.9Å); 10, Horse deoxy (2dhb, 2.8 Å).

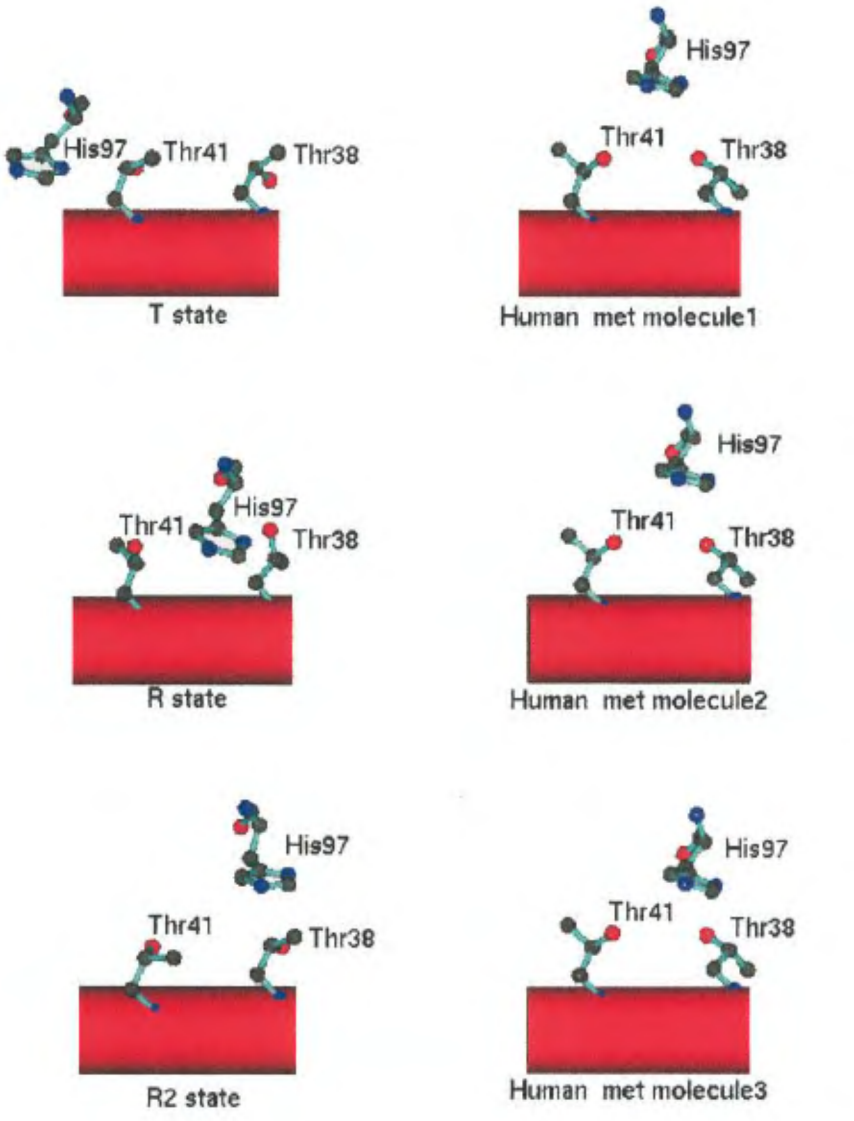

Figure 3. Switch region in the *T*, *R*, *R*2 and met states. The figure was generated using Molscript[27].

Angles (°) θ_1 (upper right) and θ_2 (lower left) that define the relation between pairs of tetramers (Figure 2). The translation (Å), the angles (°) that define the direction of rotation axis and a point (Å) on rotation axis are also given in lower left. The numbering of structures is the same as that in Table 2. See text for details

1	2	3	4	5	6	7	8	9	10
–	1.8	3.4	3.1	4.0	2.7	3.8	7.2	8.1	7.8
3.6 (–0.5) 33.2 90.0 56.8 –18.9 –2.1 –7.0	–	1.8	1.8	4.5	1.5	2.8	7.6	8.4	7.9
6.8 (–1.6) 49.6 90.0 40.4 –22.5 –5.7 –7.4	3.6 (–0.4) 67.8 90.0 22.2 –26.3 –8.7 –5.2	–	0.9	6.1	1.0	1.6	7.2	7.8	7.3
6.2 (–1.4) 64.9 90.0 25.1 –25.2 –13.5 –5.8	3.6 (0.3) 80.7 90.0 9.3 –0.3 23.8 –2.3	1.8 (–0.7) 8.2 90.0 81.8 –13.4 13.0 –2.3	–	6.2	0.5	1.0	6.5	7.2	6.6
8.0 (–1.2) 57.6 90.0 32.4 –25.1 6.0 6.8	8.9 (–0.9) 82.5 90.0 7.5 –28.7 5.9 2.2	12.2 (–1.1) 89.7 90.0 0.3 –0.0 1.1 0.3	12.4 (–1.2) 81.6 90.0 8.4 –28.8 –1.2 2.5	–	5.9	7.3	12.4	12.5	12.1
5.4 (–0.9) 62.4 90.0 27.6 –24.9 –14.8 –5.7	3.0 (–0.3) 75.6 90.0 14.4 –0.6 24.5 –3.0	2.0 (–0.6) 12.6 90.0 77.4 –13.3 –8.8 2.5	0.9 (0.5) 88.1 90.0 1.9 –0.0 10.1 0.4	11.8 (0.8) 84.9 90.0 5.1 –0.2 3.7 –2.4	–	1.4	6.5	7.2	6.8
8.0 (–1.0) 72.7 90.0 17.3 –26.9 –12.4 –4.4	5.6 (0.1) 81.8 90.0 8.2 –0.3 14.7 –2.4	3.2 (–0.4) 47.6 90.0 42.4 –6.2 12.0 –7.5	2.0 (–0.2) 81.6 90.0 8.4 0.0 –2.6 –2.4	14.6 (1.0) 86.4 90.0 3.6 –0.0 3.4 –2.1	2.8 (0.3) 73.8 90.0 16.2 0.2 –3.5 1.6	–	5.7	6.3	5.7
14.4 (2.0) 54.0 90.0 36.0 –6.3 14.3 –8.2	15.2 (1.3) 39.6 90.0 50.4 –9.8 13.8 –7.8	14.4 (0.9) 25.8 90.0 64.2 –12.5 13.8 –5.8	13.0 (1.6) 29.4 90.0 60.6 –12.2 11.6 –6.2	24.8 (3.1) 61.4 90.0 28.6 –5.4 6.8 –7.8	13.0 (1.9) 18.1 90.0 71.9 –12.9 –14.7 3.8	11.4 (1.2) 18.6 90.0 71.4 32.0 16.3 3.6	–	0.9	1.2
16.2 (2.4) 56.2 90.0 33.8 –5.2 13.2 –8.1	16.8 (1.7) 43.1 90.0 46.9 –8.4 13.1 –8.2	15.7 (1.4) 30.8 90.0 59.2 –11.2 13.5 –6.8	14.4 (2.0) 33.7 90.0 56.3 –10.6 11.3 –7.5	25.0 (3.4) 61.2 90.0 28.8 –4.8 6.6 –7.8	14.4 (2 .4) 22.6 90.0 67.4 –11.7 –13.9 5.2	12.6 (1.7) 25.0 90.0 65.0 29.8 16.2 2 .8	1.8 (0.3) 67.0 90.0 23.0 2.1 3.4 –6.9	–	0.8
15.6 (2.3) 61.5 90.0 28.5 –4.0 11.7 –7.4	15.8 (1.6) 47.2 90.0 42.8 –7.3 12.1 –8.1	14.6 (1.3) 34.6 90.0 55.4 –10.4 12.4 –7.2	13.2 (1.9) 38.8 90.0 51.2 –9.5 9.5 –7.6	24.2 (3.2) 64.4 90.0 25.6 –3.6 5.8 –7.6	13.6 (2.3) 28.1 90.0 61.9 –10.5 –12.0 5.6	11.4 (1.7) 30.8 90.0 59.2 28.2 15.6 3.5	2.4 (0.1) 66.3 90.0 23.7 –2.1 1.5 4.3	1.6 (0.1) 15.7 90.0 74.3 –11.5 18.7 3.6	–

tacts with an interatomic distance of 4 Å or less in human oxyhaemoglobin. No such contacts exist in met and *R*2 structures.

The results presented above show that the three crystallographically independent molecules in human methaemoglobin crystals have structures intermediate between the *R* and *R*2 structures, with different levels of closeness with one or the other of the latter. During the period when this communication was being prepared, three crystal structures of bovine carbonmonoxyhaemoglobin were reported[10]. The molecule in one of the three is very similar to human haemoglobin *R*2 structure, while those in the other two have subunit arrangements intermediate between those in the *R* and *R*2 structures. The three crystals were, however, grown under different conditions. In the present work, haemoglobin molecules with different degrees of closeness to *R* and *R*2 states are observed in the same crystal. Thus, haemoglobin appears to have several relaxed states with varying degrees of similarity among them.

1. Perutz, M. F., Wilkinson, A. J., Paoli, M. and Dodson, G. G., *Annu. Rev. Biophys. Biomol. Struct.*, 1998, **27**, 1–34.
2. Tame, J. R. H., *Trends Biochem. Sci.*, 1999, **24**, 372–377.
3. Monod, J., Wyman, J. and Changeux, J. P., *J. Mol. Biol.*, 1965, **12**, 88–118.
4. Perutz, M. F., *Nature*, 1970, **228**, 726–734.
5. Bolton, W. and Perutz, M. F., *Nature*, 1970, **228**, 551–552.
6. Perutz, M. F., Muirhead, H., Cox, J. M. and Goaman, L. C. G., *Nature*, 1968, **219**, 131–139.
7. Kroeger, K. E. and Kundrot, C. E., *Structure*, 1997, **5**, 227–237.
8. Silva, M. M., Rogers, P. H. and Arnone, A., *J. Biol. Chem.*, 1992, **267**, 17248– 17256.
9. Smith, F. R. and Simmons, C., *Proteins: Struct. Funct. Genet.*, 1994, **18**, 295–300.
10. Mueser, T. C., Rogers, P. H. and Arnone, A., *Biochemistry*, 2000, **39**, 15353–15364.
11. Shaanan, B., *J. Mol. Biol.*, 1983, **171**, 31–59.
12. Fermi, G., Perutz, M. F. and Shaanan, B., *J. Mol. Biol.*, 1984, **175**, 159–174.
13. Baldwin, J. M., *J. Mol. Biol.*, 1980, **136**, 103–128.
14. Vasquez, G. B., Ji, X., Fronticelli, C. and Gilliland, G. L., *Acta Crystallogr. D*, 1998, **54**, 355–366.
15. Brzozowski, A. *et al.*, *Nature*, 1984, **307**, 74–76.
16. Liddington, R., Derewenda, Z., Dodson, E., Hubbard, R. and Dodson, G., *J. Mol. Biol.*, 1992, **228**, 551–579.
17. Baldwin, J. and Chothia, C., *J. Mol. Biol.*, 1979, **129**, 175–220.
18. Otwinowski, Z. and Minor, W., *Methods Enzymol.*, 1997, **276**, 307–325.
19. Navaza, J., *Acta Crystallogr. A.*, 1994, **50**, 157–163.
20. Ladner, R. C., Heidner, E. J. and Perutz, M. F., *J. Mol. Biol.*, 1977, **114**, 385–414.
21. Brunger, A. T. *et al.*, *Acta Crystallogr. D*, 1998, **54**, 905–921.
22. Jones, T. A., *J. Appl. Crystallogr.*, 1978, **11**, 268–272.
23. Vijayan, M., *Computing in Crystallography* (eds Diamond, S. *et al.*), Indian Academy of Sciences, Bangalore, 1980, pp. 19.01–19.26.
24. Laskowski, R. A., MacArthur, M. W., Moss, D. S. and Thornton, J. M., *J. Appl. Crystallogr.*, 1993, **26**, 283–291.
25. Cohen, G. E., *J. Appl. Crystallogr.*, 1997, **30**, 1160–1161.
26. Kartz, D. S., White, S. P., Huang, W., Kumar, R. and Christianson, D. W., *J. Mol. Biol.*, 1994, **244**, 541–553.
27. Kraulis, P. J., *J. Appl. Crystallogr.*, 1991, **24**, 946–950.

ACKNOWLEDGEMENTS. Intensity data were collected at the X-ray Facility for Structural Biology supported by Department of Science and Technology (DST) and the Department of Biotechnology (DBT), Government of India. The computations were carried out at the Supercomputer Education and Research Centre, Indian Institute of Science, Bangalore and the DBT supported Graphics Facility. Financial support from the Council of Scientific and Industrial research (CSIR), India, is acknowledged. We thank G. Ramachandriah for help in preparing figures.

Received 24 July 2001, revised accepted 18 September 2001

Antibody and nucleic acid probe-based techniques for detection of sugarcane streak mosaic virus causing mosaic disease of sugarcane in India

M. Hema[†], H. S. Savithri* and P. Sreenivasulu[†,]**

[†]Department of Virology, Sri Venkateswara University, Tirupati 517 502, India
*Department of Biochemistry, Indian Institute of Science, Bangalore 500 012, India

Double antibody sandwich-enzyme linked immunosorbent assay (DAS-ELISA) and direct antigen coating (DAC)–ELISA tests were evaluated for detection of sugarcane streak mosaic virus (SCSMV-AP), a new member of *Tritimovirus* genus in the family Potyviridae, in leaf extracts, sugarcane juice and purified virus. The virus was detected up to 1/3125 and 1/625 dilutions in infected sugarcane leaf, 5 µl and 10 µl/well in sugarcane juice, 1/3125 and 1/3125 dilutions in infected sorghum leaf and 10 ng and 50 ng/ml for purified virus in DAS-ELISA and DAC-ELISA tests, respectively. A cDNA clone pSCSMV-AP (495 bp) specific to SCSMV-AP was selected as diagnostic ^{32}P and DIG (digoxigenin) probe. In slot-blot hybridization analysis, ^{32}P and DIG probes reacted with total nucleic acid extracts from infected sugarcane leaf (10^{-5} and 10^{-4}), infected sugarcane juice (10^{-3} and 10^{-4}) and infected sorghum leaf (10^{-5} and 10^{-5}). With both the probes the virus was detected in purified virus up to 50 pg and viral RNA up to 1 pg level. DAS-ELISA appears to be sensitive and ideal for routine large-scale detection of virus in small leaf tissue and cane juice samples of sugarcane. Nucleic acid-based tests could be useful in screening of sugarcane germplasm.

SUGARCANE (*Saccharum officinarum* L.) is one of the most important commercial crops in the world. The viruses known to naturally infect the crop are sugarcane

**For correspondence. (e-mail: pothursree@yahoo.com)